6TH INTERNATIONAL ELECTRONIC CONFERENCE ON SENSORS AND APPLICATIONS

Modeling the nonlinear properties of ferroelectric materials in ceramic capacitors for the implementation of sensor functionalities in implantable electronics

Yves Olsommer, Frank R. Ihmig and Carsten Müller

Fraunhofer IBMT

Fraunhofer Institute for Biomedical Engineering

Department of Biomedical Microsystems

Biotelemetry Group

Outline

- Introduction:
  - Implantable electronics and applications
  - Representation of the system
  - Sensor functionality of the further concept of this work
- Methods
  - Characterization of nonlinear capacitors
  - Modeling in ANSYS 2019 R2 Simplorer and Mathcad Prime 3.1
  - Measurement setup
- Results
- Conclusion
- Next steps

Retina stimulator

- Partial vision restoration for patient suffering from blindness (retinitis pigmentosa, cone rod dystrophy or choroidermia)
- The Intelligent Retinal Implant System (IRIS) II (Pixium Vision S.A., Paris, France)
- Wireless intraocular retinal implant (EPIRET3) (EPI-RET3 Team, RWTH Aachen, Germany)

Source adapted from: Pixium Vision S.A., Paris, France.

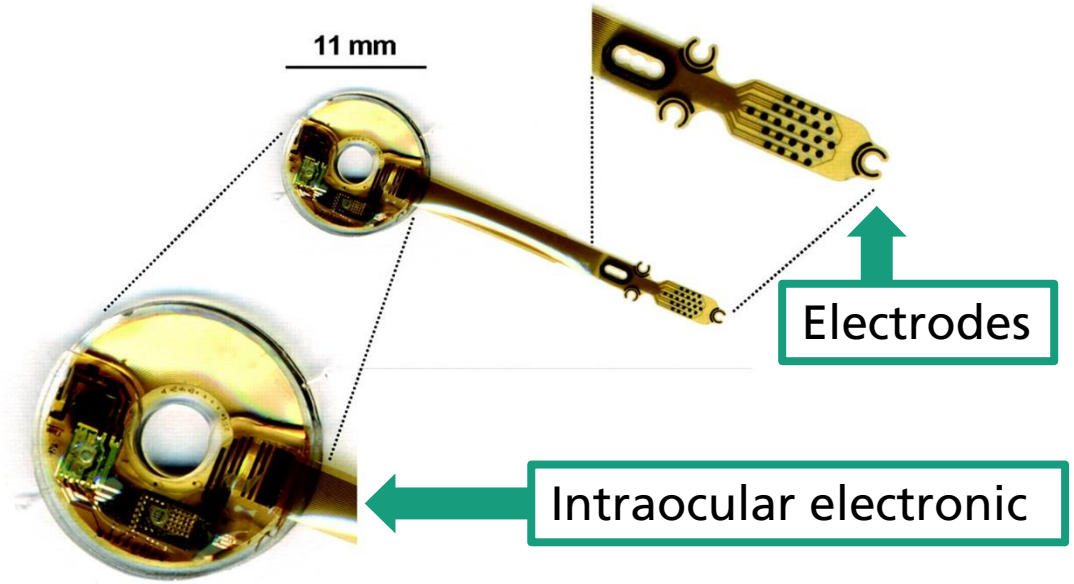

Source: Roessler, G.; Laube, T.; Brockmann, C.; Kirschkamp, T.; Mazinani, B.; Goertz, M.; Koch, C.; Krisch, I.; Sellhaus, B.; Trieu, H.K.; et al. Implantation and explantation of a wireless epiretinal retina implant device: observations during the EPIRET3 prospective clinical trial. *Invest. Ophthalmol. Vis. Sci.* **2009**, *50*, 3003–3008, doi:10.1167/iovs.08-2752.

Hypoglossal nerve stimulator

- Obstructive sleep apnea (excessive daytime somnolence, significant cardiovascular morbidity and mortality)
- Inspire Medical Systems, Inc. (Minneapolis, MN, USA)

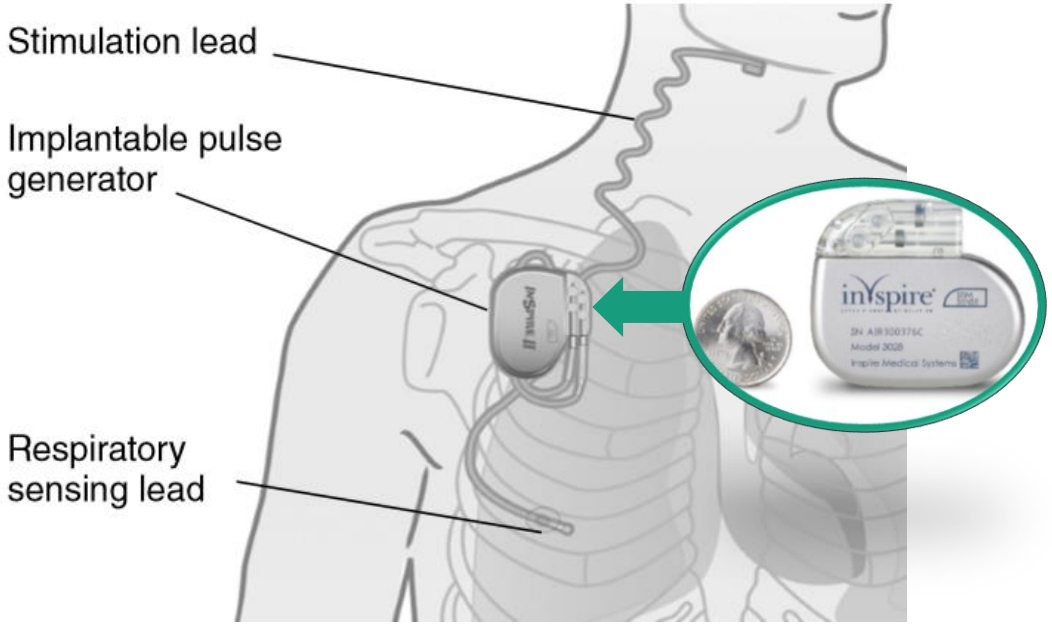

Source adapted from: Inspire Medical Systems, I. SYSTEM IMPLANT MANUAL: Inspire II Implantable Pulse Generator Model 3024. https://www.accessdata.fda.gov/cdrh_docs/pdf13/P130008D.pdf (accessed on 14 October 2019).

Source adapted from: Inspire Medical Systems, Inc. (Minneapolis, MN, USA).

- The Genio (Nyxoah, Mont-Saint-Guibert, Belgium)

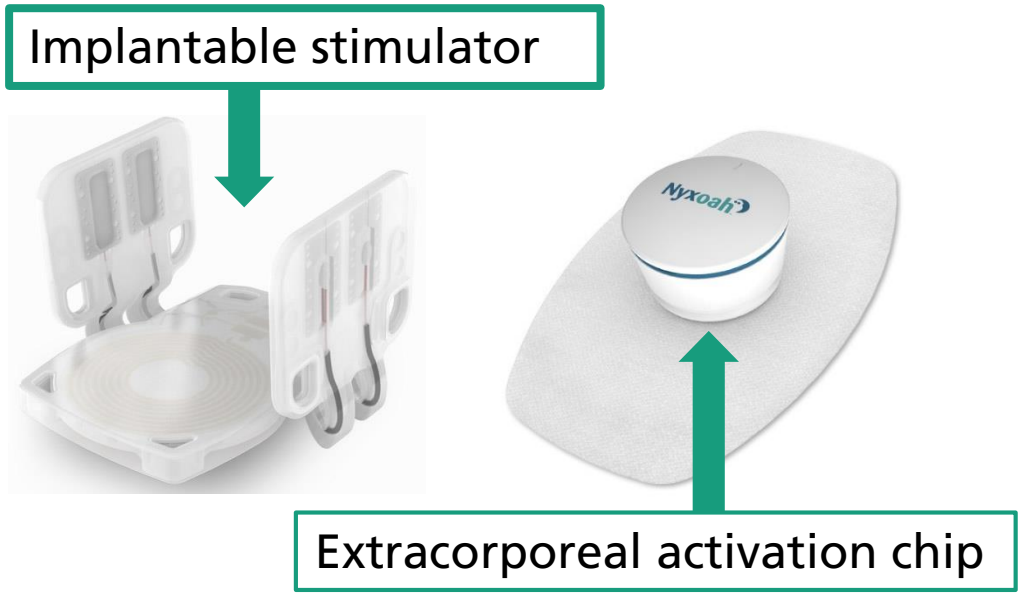

Source adapted from: Nyxoah, Mont-Saint-Guilbert, Belgium.

Vagus nerve stimulator

- Drug-resistant epilepsy, rheumatoid arthritis
- AspireSR (LivaNova PLC, London, UK)

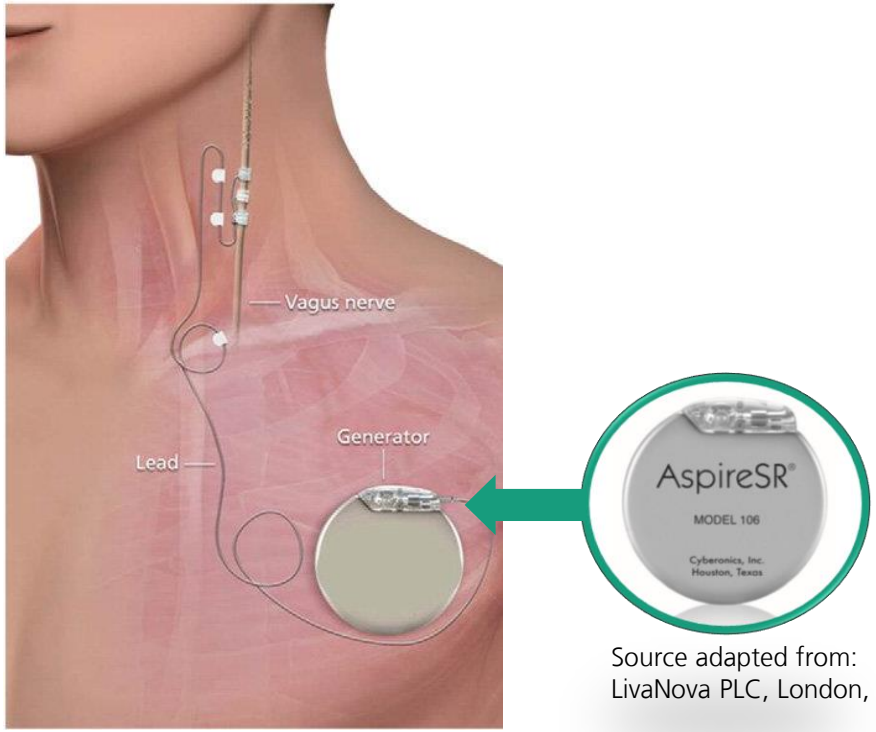

Source adapted from:
LivaNova PLC, London, UK.

Source adapted from: Verrier, R.L.; Nearing, B.D.; Olin, B.; Boon, P.; Schachter, S.C. Baseline elevation and reduction in cardiac electrical instability assessed by quantitative T-wave alternans in patients with drug-resistant epilepsy treated with vagus nerve stimulation in the AspireSR E-36 trial. *Epilepsy Behav.* **2016**, *62*, 85–89, doi:10.1016/j.yebeh.2016.06.016.

- Setpoint Medical Corporation (Valencia, CA, USA)

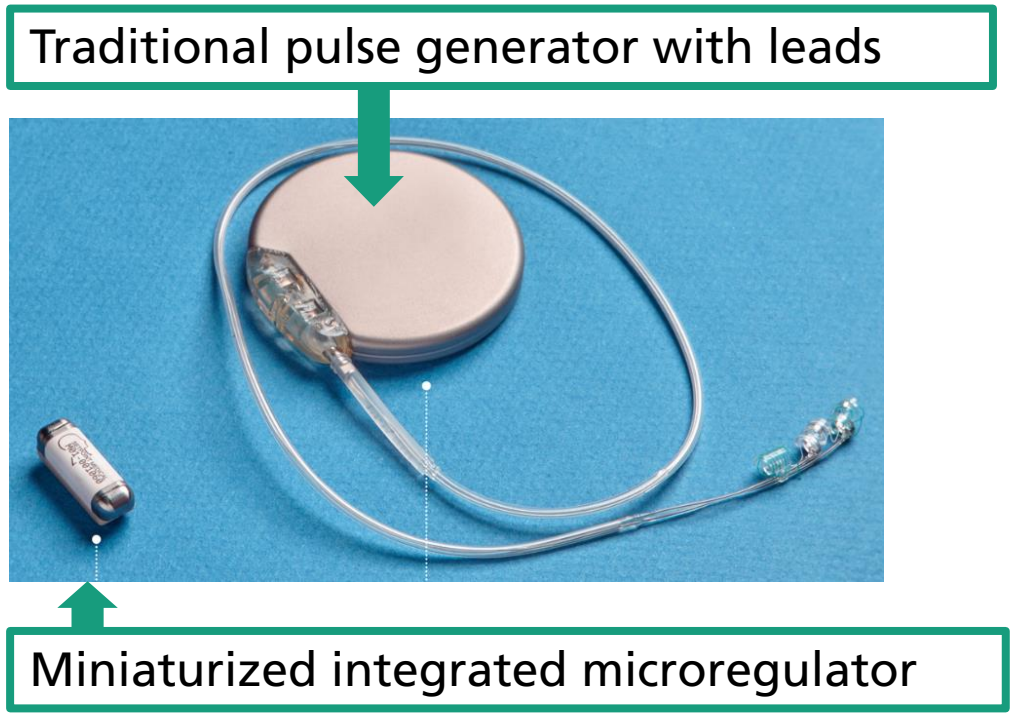

Source adapted from: Setpoint Medical, Valencia, CA, USA.

Problem

- Due to the considerable number of active electronic components, sensors, and bulky battery units in a majority of today's implantable systems for functional electrostimulation, these cannot be implanted at the location where the electrical stimulation pulses need to be applied. Therefore, the electrodes for electrostimulation are connected to the implant electronics by wires being susceptible to migration and fracture over time. In addition, malfunctions of the highly engineered implant electronics can also occur and an age-related replacement of the battery may be necessary over time [1-5].
- One solution concept is to use neither active electronic components nor sensors or batteries.
  - How functionalities can be achieved without the use of active electronic components?

1. Wolter, T.; Kieselbach, K. Cervical spinal cord stimulation: an analysis of 23 patients with long-term follow-up. *Pain Physician* **2012**, *15*, 203–212.
2. Doshi, P.K. Long-term surgical and hardware-related complications of deep brain stimulation. *Stereotact. Funct. Neurosurg.* **2011**, *89*, 89–95, doi:10.1159/000323372.
3. Taylor, R.S.; van Buyten, J.-P.; Buchser, E. Spinal cord stimulation for chronic back and leg pain and failed back surgery syndrome: a systematic review and analysis of prognostic factors. *Spine* **2005**, *30*, 152–160, doi:10.1097/01.brs.0000149199.68381.fe.
4. Kim, T.H.; Lee, P.B.; Son, H.M.; Choi, J.B.; Moon, J.Y. Spontaneous lead breakage in implanted spinal cord stimulation systems. *Korean J. Pain* **2010**, *23*, 78–81, doi:10.3344/kjp.2010.23.1.78.
5. McGreevy, K.; Williams, K.A.; Christo, P.J. Cephalad lead migration following spinal cord stimulation implantation. *Pain Physician* **2012**, *15*, E79-87.

Solution concept

- The functionalities are ensured by the use of intrinsic nonlinear properties of the already used components.
- In this way, the degree of miniaturization is increased without impairing functionality and reliability.

Representation of the system

- Representation of the inductively coupled system for energy transmission:
  - Extracorporeal primary side worn by the patient which provides the inductive energy supply
  - Secondary side implanted in the patient which converts the inductively received energy into stimulation pulses

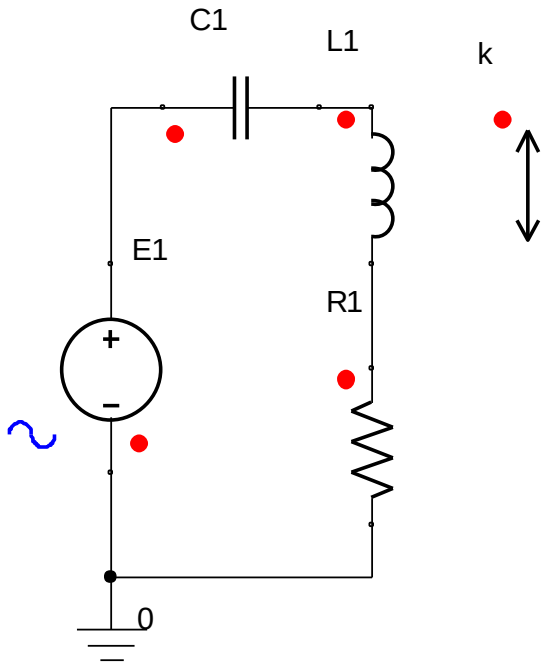

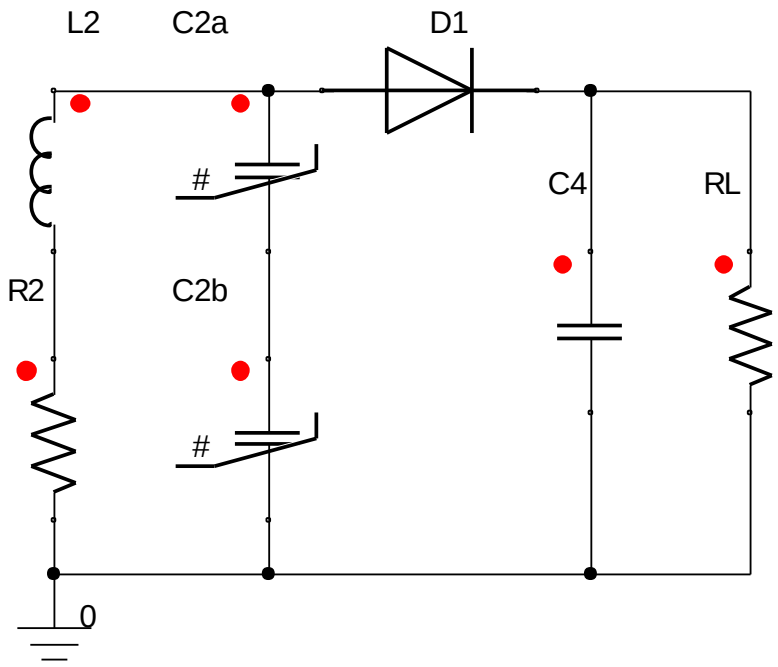

Sensor functionality of the further concept of this work

- Embedded sensor functionality and energy control concept resulting from the nonlinear capacitance

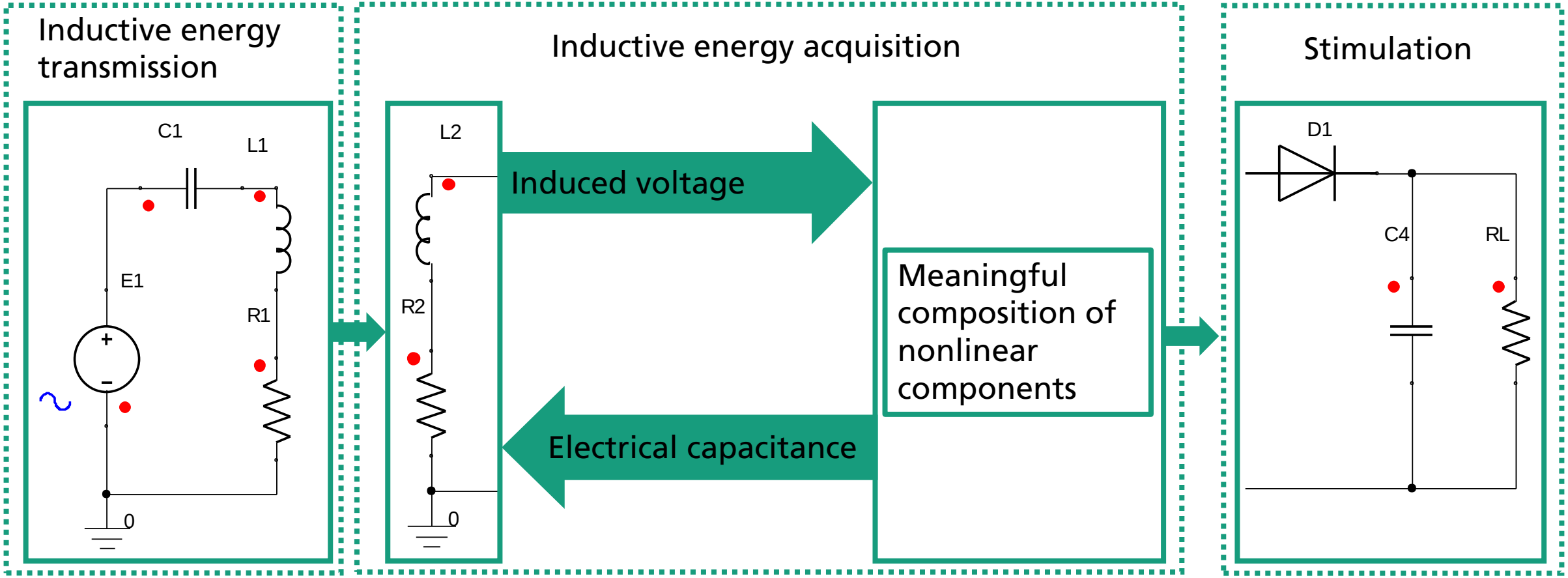

Characterization of nonlinear capacitors

- Capacitor: 100 nF, +80 %, -20 %, 25 V, Y5V, 0608
- Measurement equipment:
  - Precision impedance analyzer Agilent 4294A & test fixture Agilent 16034E
- Measurement settings:
  - AC component: 375 kHz, ±5 mV
  - Bias voltage: from –40 V to +40 V (C2a+ and C2b+) and from +40 V to –40 V (C2a- and C2b-)

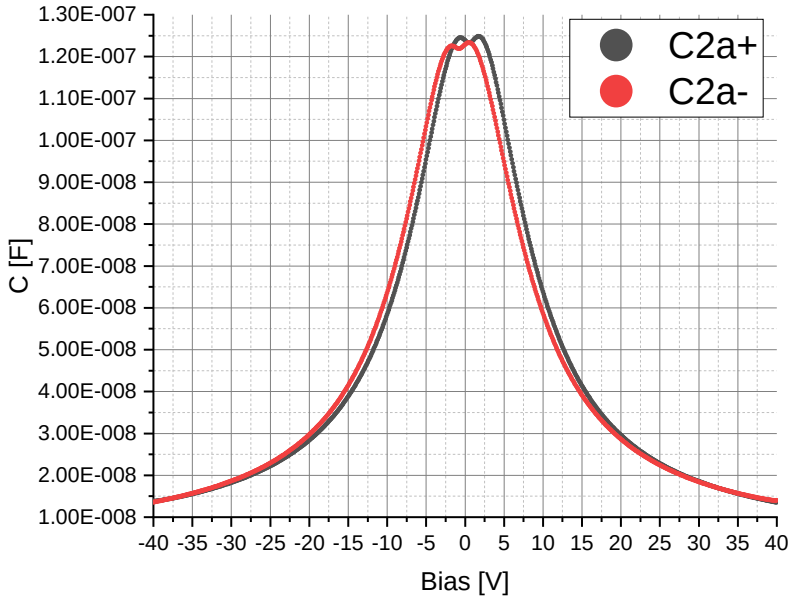

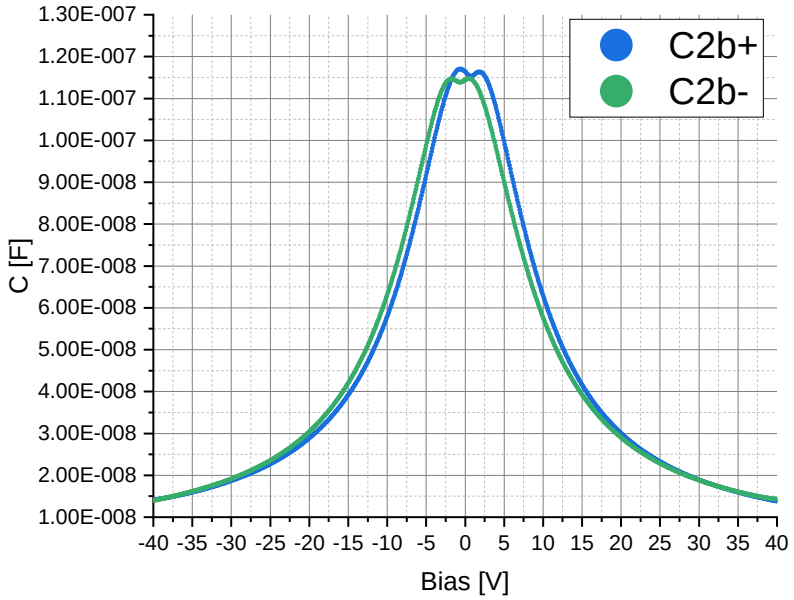

Characterization of nonlinear capacitors

- Averaged capacitance of $C2a_+$ and $C2a_-$ (C2a) and $C2b_+$ and $C2b_-$ (C2b) over the entire bias voltage range
- Hysteresis losses in Mathcad Prime 3.1 and ANSYS 2019 R2 Simplorer were neglected

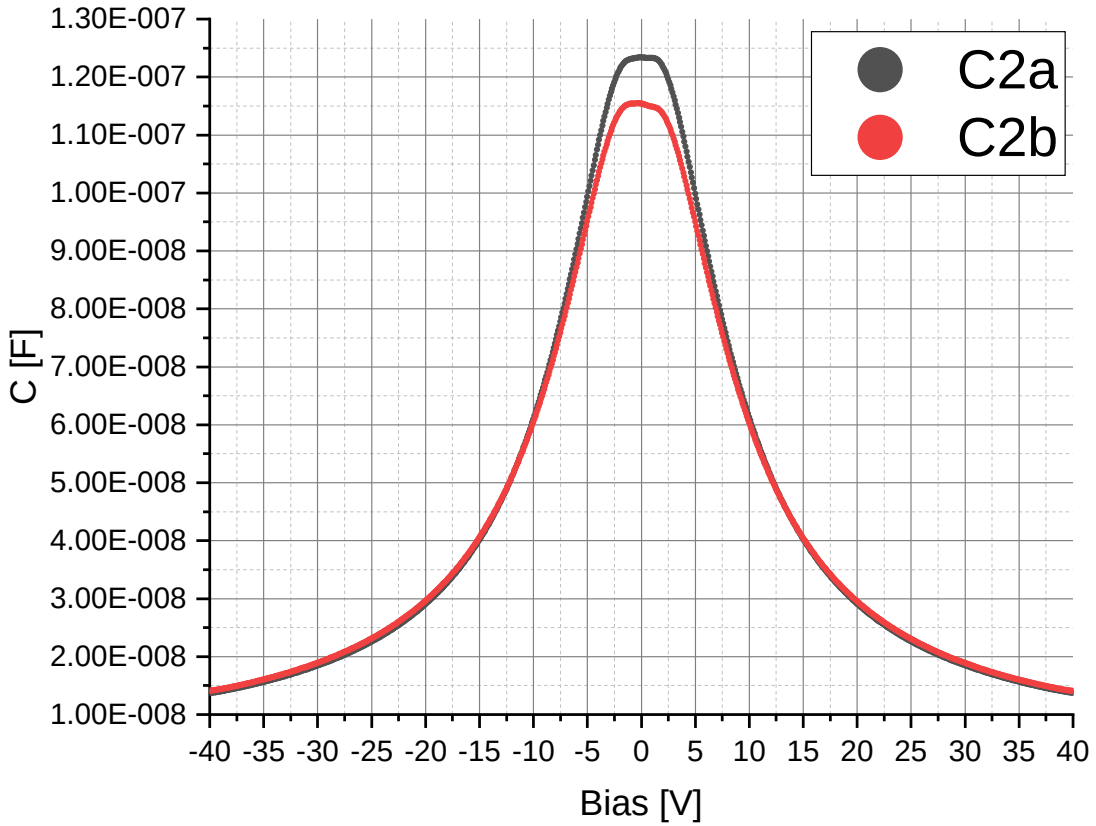

Modeling in ANSYS 2019 R2 Simplorer

- Methods: Adaptive Trapezoid-Euler, Euler and Trapezoid with constant and adaptive step width
- The amplitude of the sinusoidal excitation E1 was varied at a coupling factor of 1%

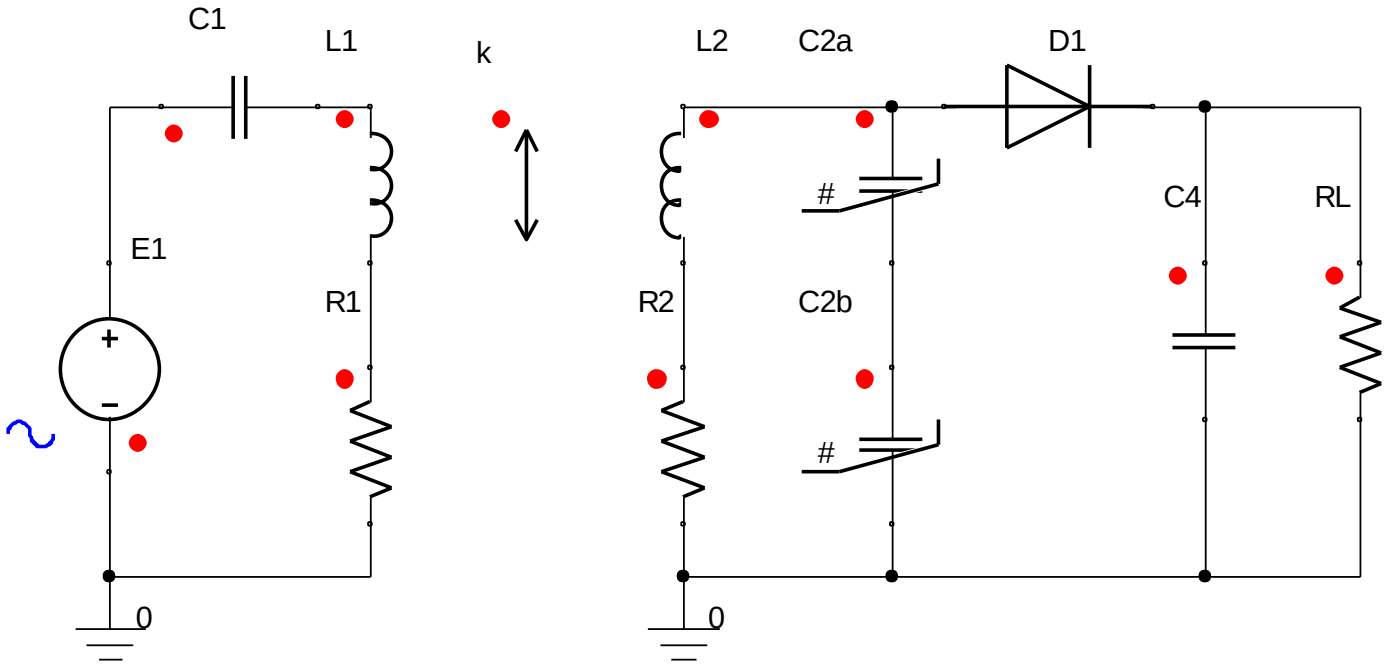

Modeling in Mathcad Prime 3.1

- Differential equations of first order:
  - $L_1 \cdot \frac{d}{dt} i_{L1}(t) + R_1 \cdot i_{L1}(t) + k \cdot \sqrt{L_1 \cdot L_2} \cdot \frac{d}{dt} i_{L2}(t) + u_{C1}(t) = u_1\left(t, A_{mp}, \omega\right)$
  - $i_{L1}(t) = C_1 \cdot \frac{d}{dt} u_{C1}(t)$
  - $L_2 \cdot \frac{d}{dt} i_{L2}(t) + R_2 \cdot i_{L2}(t) + k \cdot \sqrt{L_1 \cdot L_2} \cdot \frac{d}{dt} i_{L1}(t) = u_{C2a}(t) + u_{C2b}(t)$
  - $i_{C2}(t) = C_{2a}\left(u_{C2a}(t)\right) \cdot \frac{d}{dt} u_{C2a}(t)$
  - $i_{C2}(t) = C_{2b}\left(u_{C2b}(t)\right) \cdot \frac{d}{dt} u_{C2b}(t)$
  - $i_{C4}(t) = C_4 \cdot \frac{d}{dt} u_{C4}(t)$
  - $u_{C2a}(t) + u_{C2b}(t) = u_{D1}(t) + u_{C4}(t)$
  - $i_{L2}(t) + i_{C2}(t) + i_{D1}\left(u_{D1}(t)\right) = 0$
  - $i_{D1}\left(u_{D1}(t)\right) = i_{C4}(t) + i_{RL}(t)$
  - $i_{RL}(t) = \frac{u_{C4}(t)}{R_L}$

- Method:
  - Fourth order Runge-Kutta with constant step width
  - Fourth order Runge-Kutta with adaptive step width
  - Adams
  - Bulirsch-Stoer
  - Backward-Differentiation-formula
  - Radau5
- Interpolation with third order B-Spline functions

Measurement setup

- Primary side which provides the inductive energy supply

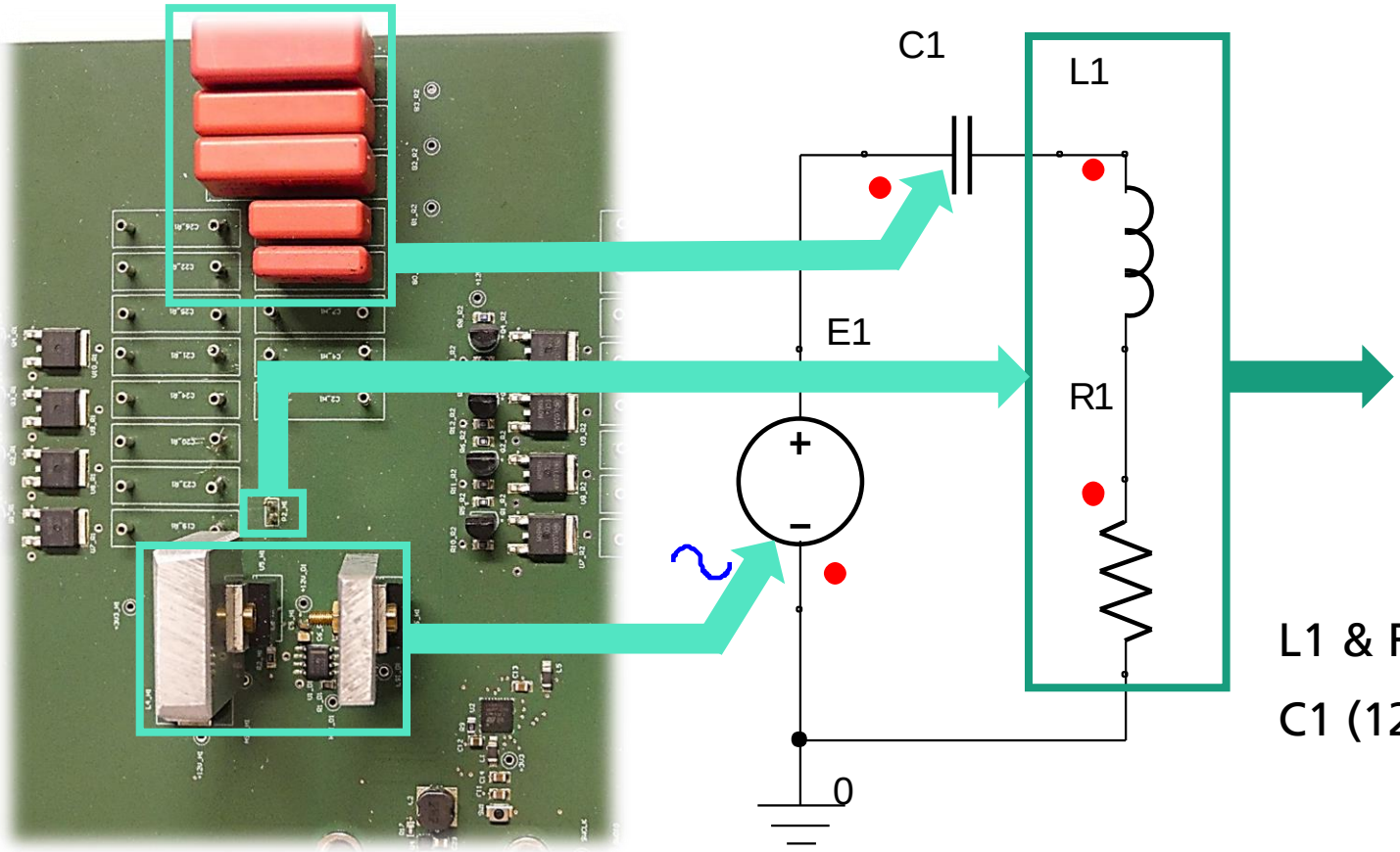

L1 & R1 (14.53 µH, 0.4 Ω, Würth Elektronik)

C1 (12.45 nF, WIMA, FKP1, 2 kV)

Measurement setup

- Secondary side which converts the inductively received energy into stimulation pulses

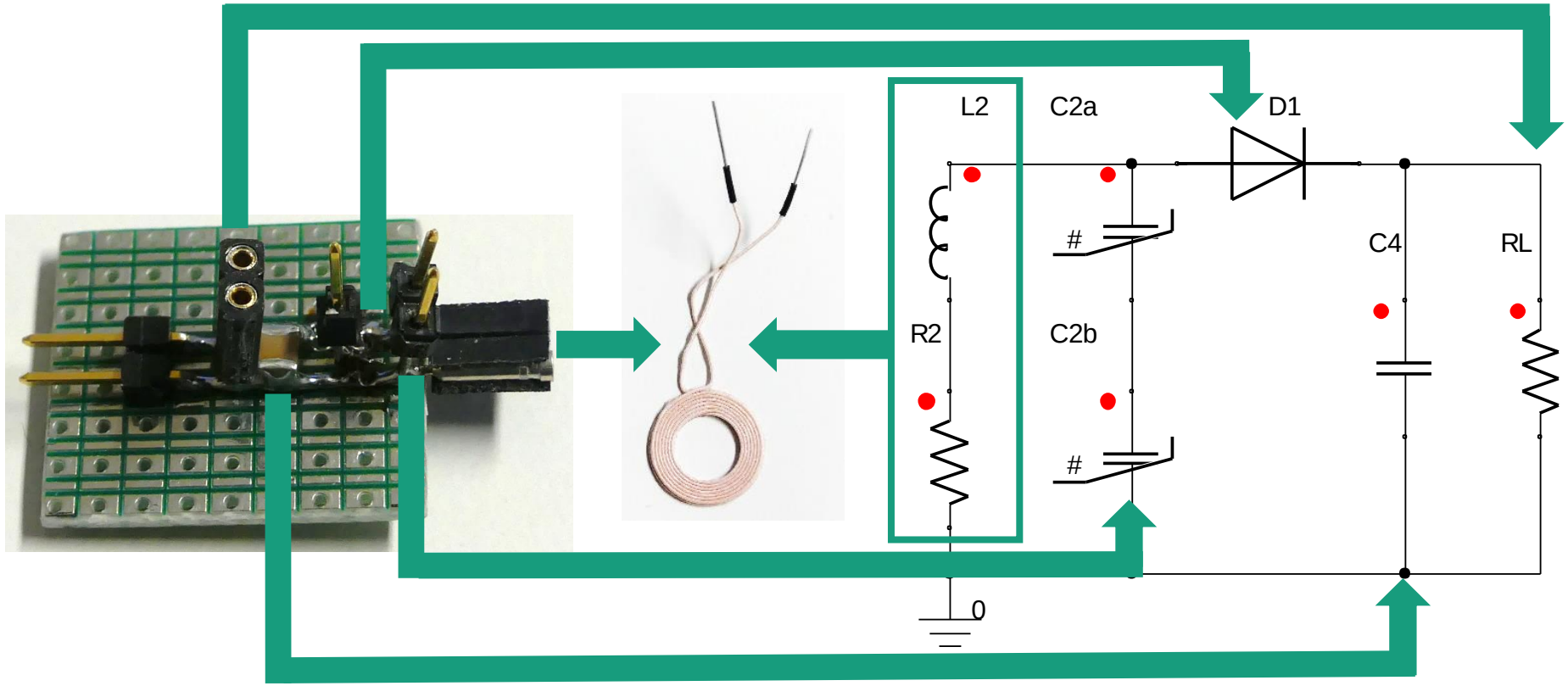

L2 & R2 (3.76 µH, 0.3 Ω, Würth Elektronik)

D1 (MULTICOMP, 1N4148WS.)

RL (1 kΩ, ±1 %)

C2a & C2b (100 nF, +80 %, -20%, Y5V, 25 V, 0608)

C4 (4.7 µF, 50 V)

Measurement setup

- Different induced voltages across the capacitors C2a and C2b were set by changing the distance between the inductance L1 and L2 on the primary and secondary side

Secondary side: L2 & R2 (3.76 µH, 0.3 Ω, Würth Elektronik)

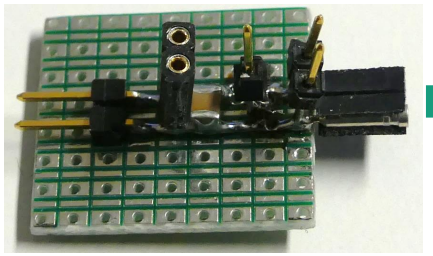

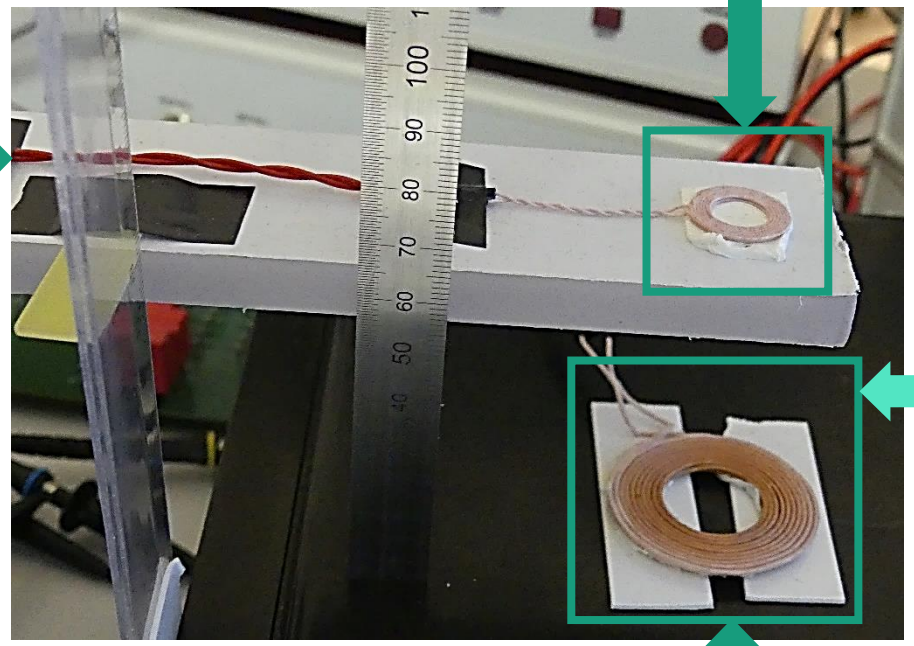

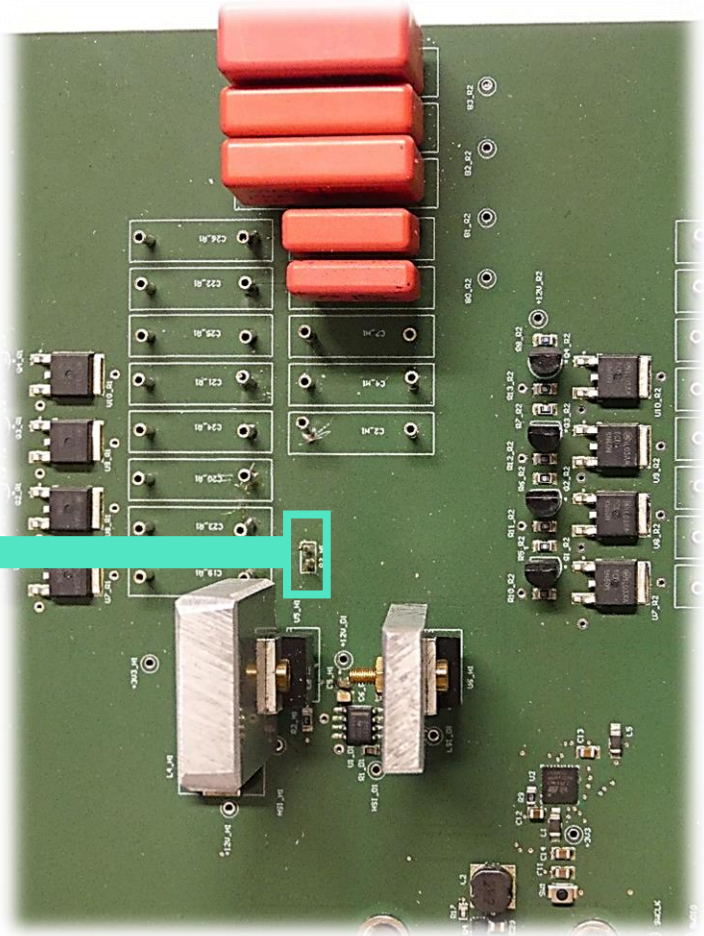

Primary side: L1 & R1 (14.53 µH, 0.4 Ω, Würth Elektronik)

Results

- $s = \sqrt{\frac{1}{N}\sum(M - B)^2}$
- B corresponds to the calculated and M to the measured mean value of the voltage Uc4Mean at the load. The squared difference of M and B was summed over an equal range of the root mean square voltage Uc2RMS across the capacitors C2a and C2b from 2.5 V to 26.9 V with a step width of 1 mV and subsequently divided by the number of steps N.
- All methods with a minimum deviation of 0.67 V provide the same time-related curve of the voltage Uc4 at the load RL
- This minimum deviation is due to:
  - Measurement error of the components
  - Neglect of hysteresis losses

Method	50k Points	500k Points	5M Points
Adams	0.67 V	0.67 V	0.67 V
Bulirsch-Stoer	0.67 V	0.67 V	0.67 V
Runge-Kutta [1]	4.51 V	0.67 V	0.67 V
Runge-Kutta [2]	0.67 V	0.67 V	0.67 V
BDF [4]	0.67 V	0.67 V	0.67 V
Radau5	0.67 V	0.67 V	0.67 V
Euler [1]	22.22 V	22.19 V	20.47 V
Trapezoid [1]	17.37 V	0.67 V	0.67 V
ATE [1,3]	21.90 V	2.87 V	0.67 V
Euler [2]	22.22 V		
Trapezoid [2]	0.67 V		
ATE [2,3]	14.16 V		

1 With constant step size; 2 With variable step size; 3 Adaptive Trapezoid-Euler; 4 Backward-Differentiation-Formula.

Results

- Comparison between calculations with a deviation of 0.67 V and measurements
- In the range of Uc2RMS greater than approx. 14 V, the calculated Uc4Mean values are higher than the measured values
- Above a certain voltage across the capacitors C2a and C2b, the relationship between the voltages Uc4Mean and Uc2RMS changes
- A possible explanation for this would be that the models are based on the mean value of the hysteresis curve of the capacitors C2a and C2b and thus the associated hysteresis losses are neglected in the calculations.

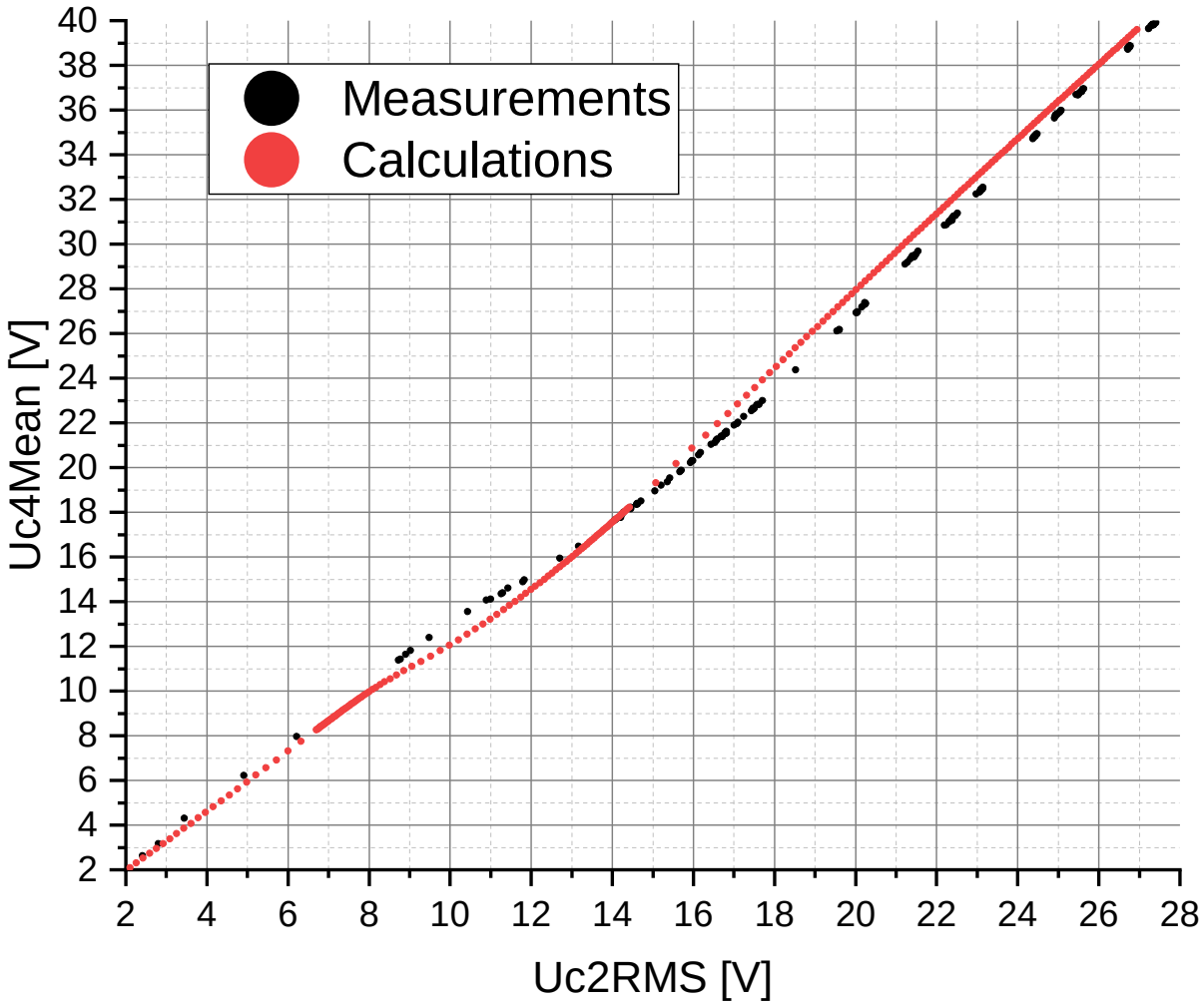

Results

- Comparison between the measurements (black) and calculation with ANSYS (blue) and Mathcad (red)
- The threshold value to be reached by Uc2RMS for triggering the nonlinear behavior on the voltage Uc4 is lower in the calculations than in the measurements. This is why the high peak of the calculated curve occurs in the measured curve only if a higher Uc2RMS compensating the hysteresis losses is applied.

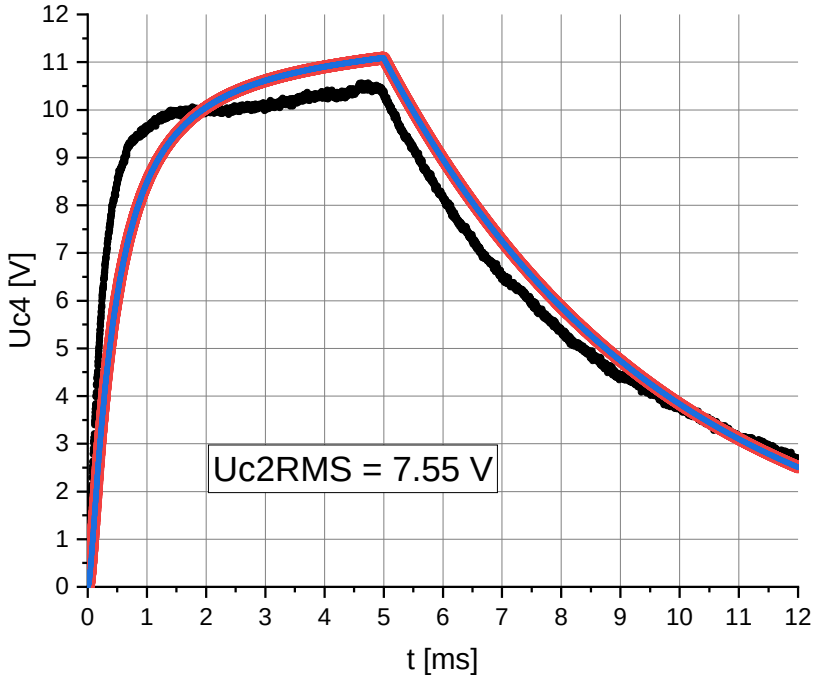

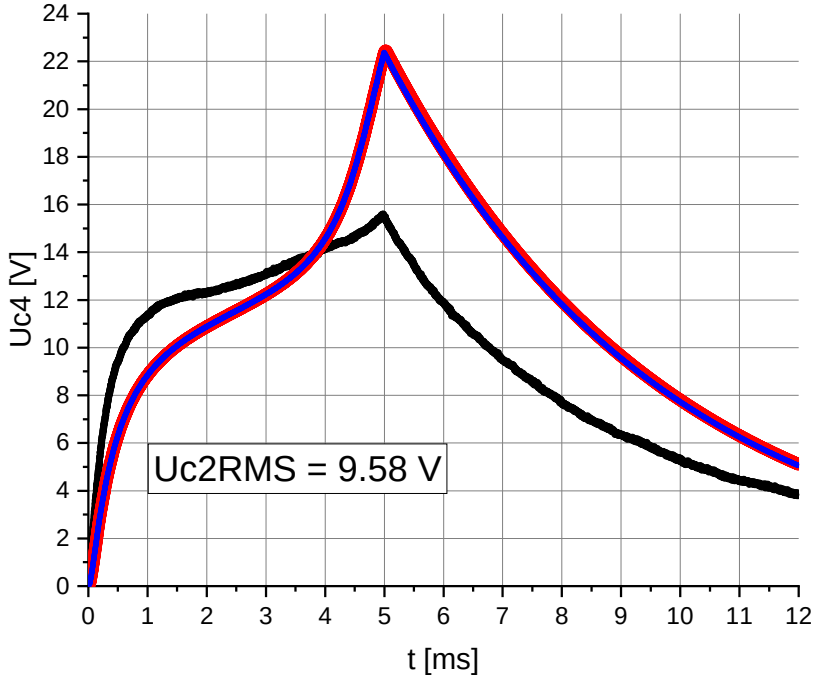

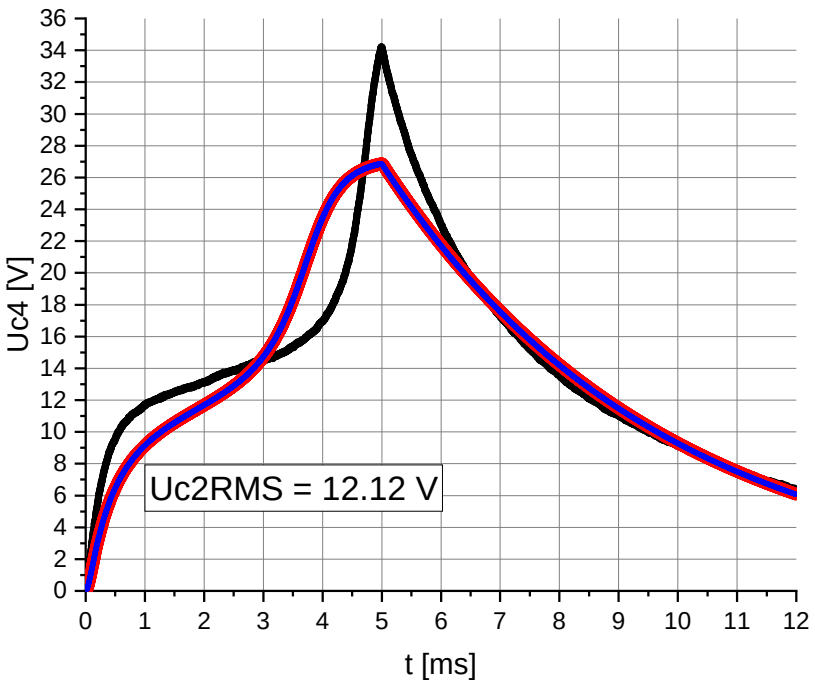

Conclusion

- ANSYS 2019 R2 Simplorer:
  - Euler method is inaccurate
  - Adaptive Trapezoid-Euler method with a resolution of 5M points and Trapezoid method with a resolution of 5M points and with adaptive step width are memory-consuming (approx. 390-444 GB)
  - Trapezoid method with constant step width and a resolution of 500k points is preferable
- Mathcad Prime 3.1:
  - Fourth order Runge-Kutta method with constant step width and a resolution of 50k point is inaccurate
  - Fourth order Runge-Kutta with adaptive step width, Adams, Bulirsch-Stoer, Backward-Differentiation-formula, Radau5 method with a resolution of 50k points could be used
  - Particular attention should be paid to third order B-Spline functions for interpolation

Next steps

- Implement the hysteresis losses in the model
- Investigate a meaningful composition of nonlinear components, such as nonlinear capacitors, in order to allow an indirect sensing of the induced voltage necessary for the power supply of the implant electronics by means of a change in the nonlinear electrical capacitance
- Use of sensor functionality to enable embedded energy control (non-linearity of components) for implant electronics.

Funding

- This research was funded by the German Federal Ministry of Education and Research (BMBF, funding number 16SV7637K). The author is responsible for the content of this publication.

Bundesministerium für Bildung und Forschung

INTAKT